Developmental Cell *19*

Supplemental Information

Rho-Kinase Directs Bazooka/Par-3 Planar Polarity during *Drosophila* Axis Elongation

Sérgio de Matos Simões, J. Todd Blankenship, Ori Weitz, Dene L. Farrell, Masako Tamada, Rodrigo Fernandez-Gonzalez, and Jennifer A. Zallen

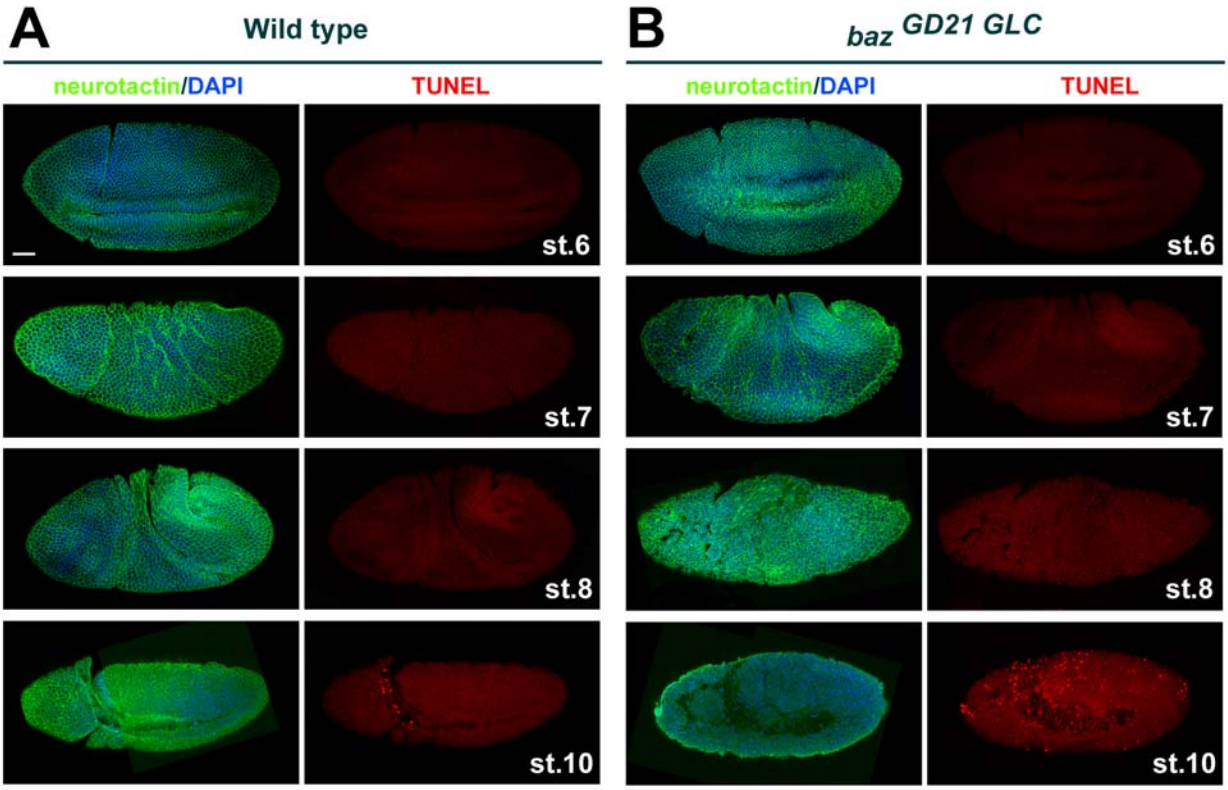

Figure S1, related to Figure 1. Apoptosis is not disrupted during germband extension in *baz* mutants

TUNEL assay in wild-type (A) and *baz*^{GD21} mutant (B) embryos at stages 6-10. Apoptotic nuclei (bright red dots) are not observed until stage 10 in both genotypes. Scale bar = 50 μm.

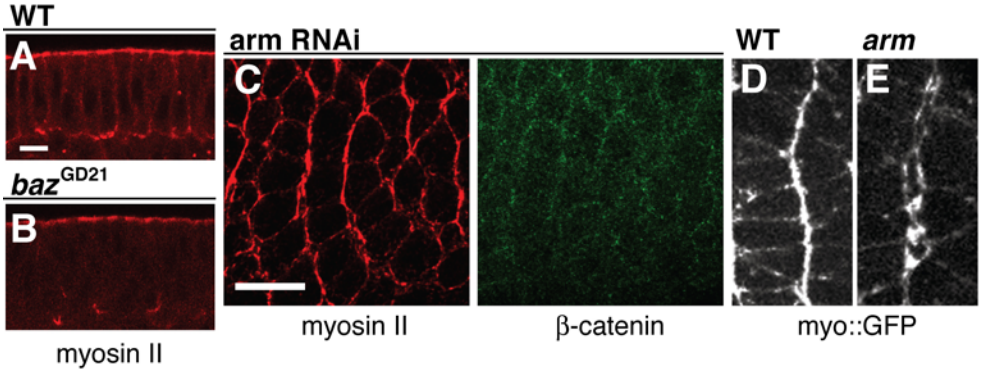

Figure S2, related to Figure 2. Arm/β-catenin is not required for myosin II planar polarity
(A,B) Cross sections of a wild-type (A) and *baz*^{GD21} mutant (B) embryos stained for myosin II (Zip heavy chain, red). Myosin II is apically localized in *baz*^{GD21} mutants as in wild type. (C) Localization of myosin II (Zip, red) and β-catenin (green) in a stage 7 embryo injected with *arm* dsRNA (4/4 embryos injected with *arm* dsRNA displayed myosin planar polarity). (D,E) Localization of myosin II (Sqh:GFP regulatory light chain) in a living wild-type (D) or *arm*^{043A06} maternal and zygotic mutant embryo (E). Myosin II planar polarity was not obviously disrupted in Arm/β-catenin mutant or dsRNA-injected embryos. Scale bars = 10 μm.

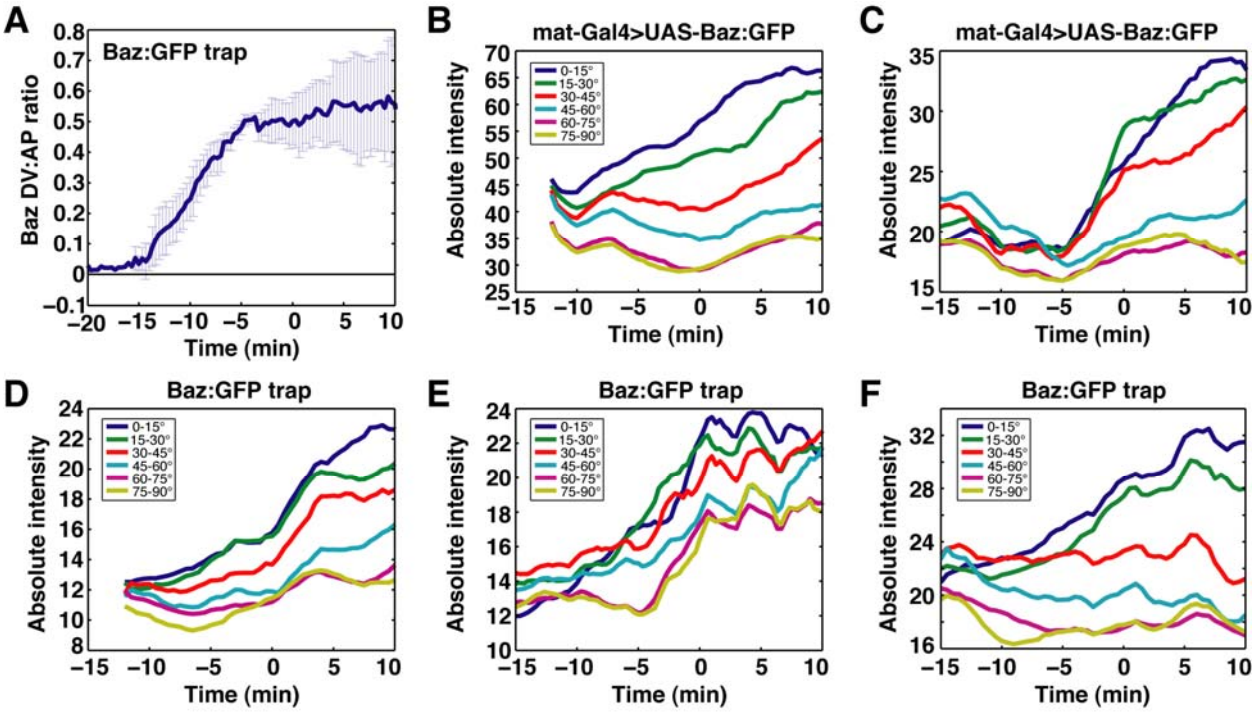

Figure S3, related to Figure 3. Baz is downregulated at AP edges and upregulated at DV edges, establishing planar polarity
Quantitation of fluorescence in time-lapse movies of embryos expressing endogenous Baz:GFP (Baz:GFP trap, A,D-F) or ectopic Baz:GFP under the control of the maternal α-tubulin Gal4 promoter (B,C). (A) The $\log_2$ ratio of Baz:GFP intensity at DV edges (oriented at ≤30° relative to the AP axis) relative to AP edges (oriented at ≥60° relative to the AP axis) was averaged across

all cells (n = 3 embryos, 610-1848 edges/embryo). An average value was obtained for each embryo and error bars indicate the standard error of the mean across embryos. t = 0 is the onset of elongation in stage 7. (B-F) Absolute edge intensities grouped by edge orientation in individual embryos expressing ectopic Baz:GFP (B,C) or endogenous Baz:GFP (D-F). Baz is first downregulated at AP edges (yellow, purple), followed by an increase in Baz apical localization that is most pronounced at DV edges (dark blue, green).

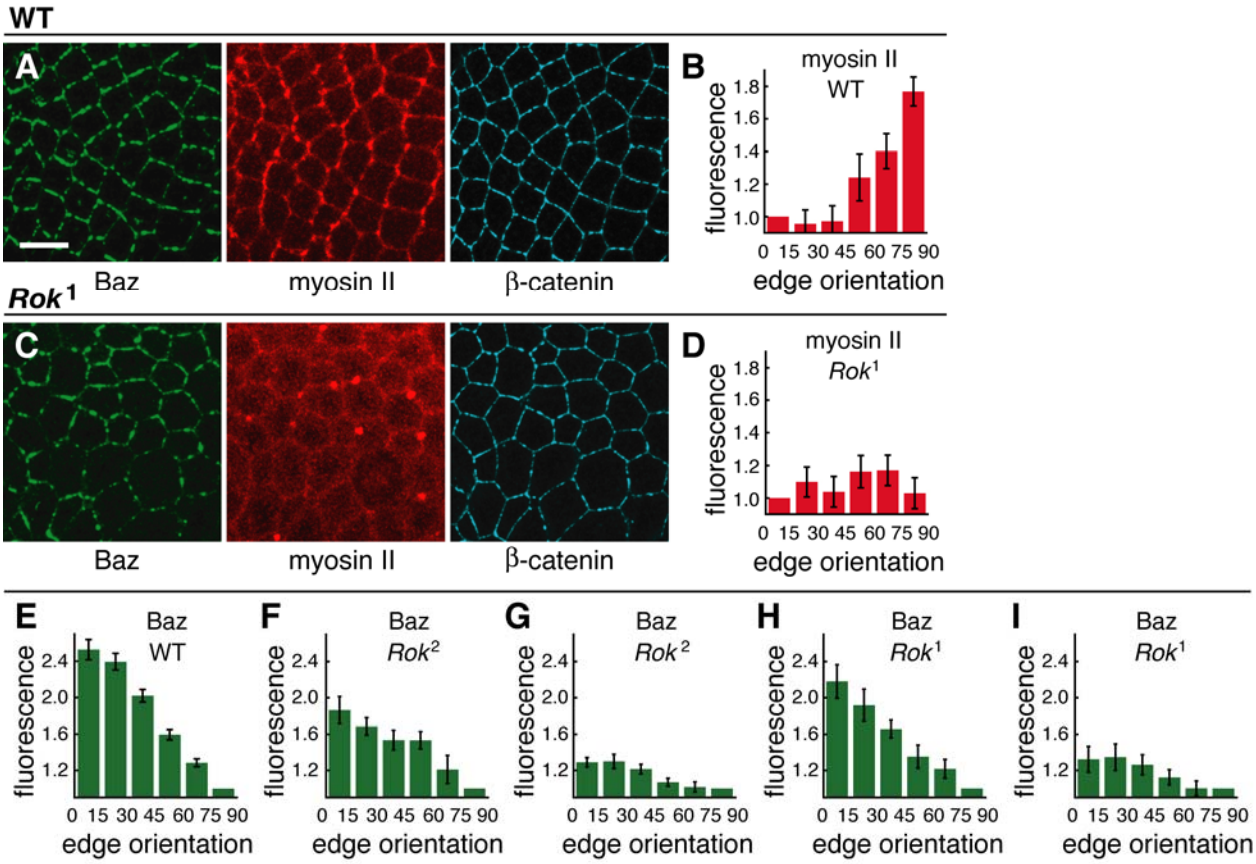

Figure S4, related to Figure 4. Rho-kinase is required for Baz and myosin planar polarity
Baz (green), myosin II (Zip heavy chain, red), and β-catenin (blue) localization in wild-type (A) and *DRok*^{1} mutant (C) embryos. Scale bar = 10 μm. (B,D) Myosin cortical localization and planar polarity were strongly reduced in *DRok*^{1} (D) compared to wild type (B) (n = 5 wild-type and 11 *DRok*^{1} mutant embryos, $P<0.001$). (E-I) Quantitation of Baz planar polarity. (E) Wild-type. (F,G) 4/12 *DRok*^{2} embryos showed partial Baz planar polarity (F), 8/12 *DRok*^{2} embryos showed a strong loss of Baz planar polarity (G) ($P<0.001$). (H,I) 6/13 *DRok*^{1} embryos showed partial Baz planar polarity (H), 7/13 *DRok*^{1} embryos showed a strong loss of Baz planar polarity (I) ($P<0.001$) (n = 13 *DRok*^{1}, 12 *DRok*^{2}, and 11 wild-type embryos). Error bars indicate the standard error of the mean across images. The two classes of *DRok*^{1} and *DRok*^{2} maternally mutant embryos are consistent with a partial zygotic rescue.

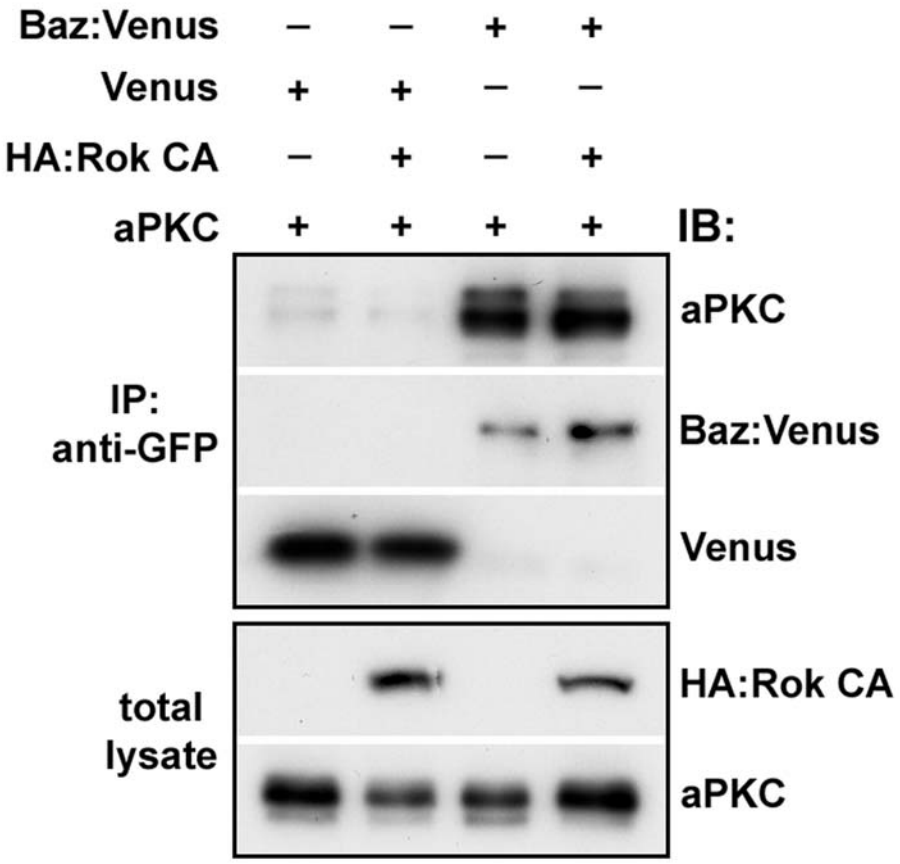

Figure S5, related to Figure 6. Rho-kinase does not disrupt the interaction between Baz and aPKC in cultured cells

Drosophila S2R+ cells were transfected with the indicated plasmids. 16 hours after transfection, cell lysates were prepared and Venus or Baz:Venus were immunoprecipitated (IP) with an anti-GFP antibody. Bound proteins were detected by immunoblotting (IB) with anti-GFP, anti-HA or anti-aPKC antibodies. aPKC did not coimmunoprecipitate with Venus alone, and aPKC co-immunoprecipitated with Baz:Venus equally efficiently in the presence or absence of Rok CA.

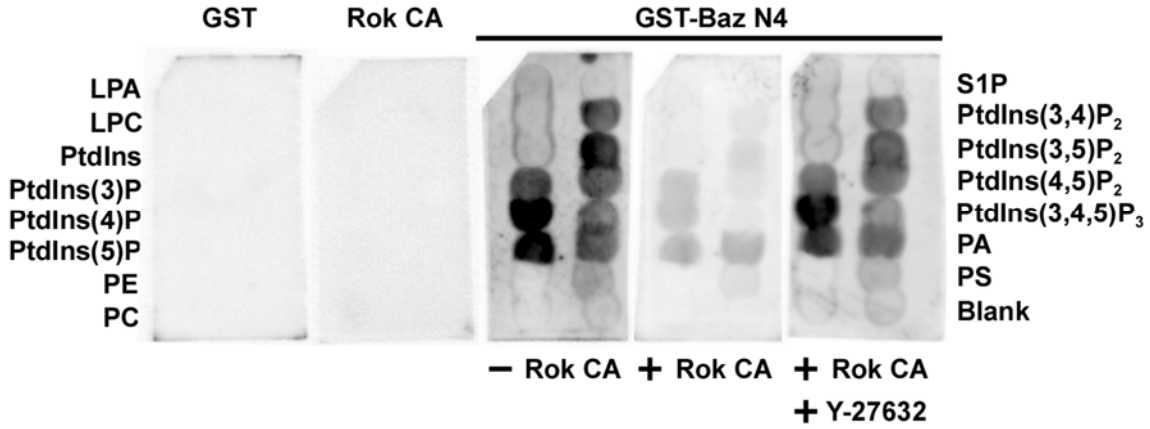

Figure S6, related to Figures 6 and 7. Phosphorylation of the Baz C-terminal domain by Rho-kinase inhibits its association with phosphoinositide membrane lipids
Lipid membrane strips were incubated with GST, GST-Rok CA alone, or GST-Baz N4, after preincubation with ATP with or without GST-Rok CA and Y-27632 as indicated. Bound proteins were detected using anti-GST antibodies. GST and GST-Rok CA did not bind to the membrane strips. LPA-lysophosphatidic acid; LPC-lysophosphocholine; PE-phosphatidylethanolamine; PC-phosphatidylcholine; S1P-sphingosine-1-phosphate; PA-phosphatidic acid; PS-phosphatidylserine.

SUPPLEMENTAL EXPERIMENTAL PROCEDURES

Fly stocks and genetics

Germline clones were generated using the FLP-DFS system with *ovo*^{D1} FRT101, *ovo*^{D2} FRT18E (Chou and Perrimon, 1996) or *ovo*^{D2} FRT19A (gift of N. Tolwinski) by heat-shocking larvae of the indicated genotypes and crossing to wild-type males. All mutations are on the X chromosome and half of the progeny of females of the following genotypes are predicted to receive a wild-type zygotic paternal contribution.

baz^{GD21} FRT19A/*ovo*^{D2} FRT19A; hs-FLP^{38}/+; GFP:Spider/+
baz^{GD21} FRT19A/*ovo*^{D2} FRT19A; hs-FLP^{38}/+; E-cadherin:GFP/+
baz^{FA50} FRT19A/*ovo*^{D2} FRT19A; hs-FLP^{38}/+; GFP:Spider/+
baz^{FA50} FRT19A/*ovo*^{D2} FRT19A; hs-FLP^{38}/+; E-cadherin:GFP/+
sqh^{1} FRT19A/*ovo*^{D2} FRT19A; hs-FLP^{38}/+; GFP:Spider/+
arm^{043A06} FRT101/*ovo*^{D1} FRT101; hs-FLP^{38}/+; sqh-sqh:GFP/+
DRok^{2} FRT18E/*ovo*^{D2} FRT18E; hs-FLP^{38}/+
DRok^{1} FRT19A/*ovo*^{D2} FRT19A; hs-FLP^{38}/+

Automated tracking

For each embryo, cells tracked together with their neighbors for ≥20 min were analyzed for neighbors lost and shrinking edge measurements and cell tracked for ≥30 min were analyzed to measure elongation. The tissue was approximated as an ellipse by calculating the inertia tensor for the collection of centers of mass of the cells. The AP length of the group of cells is the horizontal span of the ellipse

$$l = \sqrt{(L_1 \cos(\alpha))^2 + (L_2 \sin(\alpha))^2}$$

where L_1 and L_2 are the major and minor axes of the ellipse and α is the angle of the major axis with respect to the AP axis. An edge was scored as shrinking if it completely disappeared during the course of the movie. The angle assigned to each shrinking edge was the average angle in the period 3-5 min (inclusive) before the edge disappeared. Similar results were obtained using other time frames ranging from 1-10 min before edge disappearance. For each embryo, the number of shrinking edges in each 15° angular bin was divided by the total number of shrinking edges in the field of view. A percentage was obtained for each embryo and average values ± the standard error of the mean across embryos are shown.

Cell polarity measurements

Cells in the region of interest were automatically segmented with a custom image analysis program and manually corrected with an interactive user interface. Segmentation was performed on projections of multiple z-planes and channels when necessary to obtain complete cell outlines.

Edge placement was optimized by shifting edges within a confined area and selecting the position that overlies the total highest intensity pixels. Baz fluorescence intensity for each edge was measured by calculating the average pixel intensity along the edge and subtracting the background fluorescence estimated by the cytoplasmic pixel intensities at the centers of the 20 nearest cells. AP and DV intensities were defined for each cell as the average intensity of all AP edges (oriented at ≥60° relative to the AP axis) or DV edges (oriented at ≤30° relative to the AP axis) of that cell. Polarity was measured as the $\log_2$ ratio of DV intensity/AP intensity for each cell and averaged across all cells to generate a mean value for each embryo at each time point. Where polarity was analyzed in subsets of edges binned by orientation, rotating edges were assigned to the bin that reflects their current angle.

dsRNA injection

Templates to produce double-stranded RNA were generated by PCR from genomic DNA with the following primer pairs containing the T7 promoter sequence (5'-TAATACGACTCACTATAGGGAGACCAC-3') on the 5'end:
baz T7-forward 5'-AGTACGAAATGAAGGTCACCGTC-3'
baz T7-reverse 5'-TTTGTTACTGCCCTCTGCCTTCA-3'
baz 5'UTR T7-forward 5'-AATGCGCGCGTGTATGAATCACAC-3'
baz 5'UTR T7-reverse 5'-ACGACCGCATCATCATCATCGTCG-3'
arm T7-forward 5'-TCAATACAATCCACCTGATCTGC-3'
arm T7-reverse 5'-TGCAGCAGAGTAACCATCTTCTG-3'
eve T7-forward 5'-TGCCTATCCAGTCCGGATAACTCC-3'
eve T7-reverse 5'–CACACCCAGTCCGGTATAGCAGG-3'
runt T7-forward 5'–ATGGTGGCCAACAACACACAGGTC-3'
runt T7-reverse 5'–GCTTTGCTGTAGCTGGCGATCTGC-3'
Kruppel T7-forward 5'–CATGAGCACATTGGCCAACACTC-3'
Kruppel T7-reverse 5'–CTGATTGGAGTCACTGAATTTGCC -3'
PCR products were used as templates for the T7 transcription reactions with the 5X MEGAscript T7 Kit (Ambion). dsRNA was injected ventrally at 2 μg/μl in 0-1h embryos. Embryos were incubated in a humidified chamber at 25ºC for 2 h 30 min and processed for immunostaining. For analysis of the localization of Baz:GFP transgenes, endogenous Baz was knocked down by injection of dsRNAs against the *baz* open reading frame (Figure 5E) or the 5'UTR region of *baz* mRNA that was not present in the transgenes (Figure 7D-K).

Cell transfection

Drosophila S2R+ cells were maintained in Schneider's medium supplemented with 10% fetal calf serum at 25°C. Plasmid transfections were performed with CellFectin (Invitrogen). pUASp-Baz:Venus, pUASp-Baz1097-1464:Venus, pUASp-Baz905-1221:Venus, pUASp-Sqh^{E20,E21}:HA and pUASp-LimK^{T591E}:HA (this work), pUASp-GFP:Baz, pUASp-GFP:BazΔ1097-1464, pUASp-GFP:BazΔ1107-1464PHP (Krahn et al., 2010), pUASp-HA:Rok CA (Wang and Riechmann, 2007), and pUAST-Rho^{V14} (Fanto et al., 2000) were cotransfected with pAc5.1/V5-HisB-GAL4. Cells were fixed 24 h after transfection for 10 min in 4% PFA/PBS. HA-tagged proteins were detected with rat anti-HA (Roche, 1:500) and Rho^{V14} was detected with mouse anti-Rho1 (DSHB, 1:50) in blocking solution (1% BSA, 0.1% Triton X-100, 10 mM Glycine in PBS) followed by incubation with Alexa-568 secondary antibodies (Molecular Probes, 1:500).

Immunoprecipitation
S2R+ cells were cotransfected with pAc5.1/V5-HisB-GAL4 and pUASp-Venus, pUASp-Baz:Venus, pUASp-aPKC and pUASp-HA:Rok CA as described above. Protein extracts were prepared by addition of lysis buffer [50 mM Tris-HCl (pH=8), 2 mM EDTA, 150 mM NaCl, 10% glycerol, 1% Nonidet P-40, 1 mM phenylmethylsulphonyl fluoride, 10 μg/ml leupeptin, 1μg/ml pepstatin, 10μg/ml aprotinin, Phosphatase inhibitor cocktail 1 (Sigma, 1:200)] and clarified by centrifugation at 16,000Xg for 30 min at 4ºC. The soluble supernatants were incubated with mouse anti-GFP antibody (Roche, 1:200) for 1 h at 4ºC. Immunocomplexes were precipitated with Protein G-Sepharose 4B (Amersham), washed three times in lysis buffer, eluted by boiling in SDS sample buffer, and subjected to immunoblot analysis with rat anti-HA (Roche 1:2000), mouse anti-GFP (Roche 1:1000), or rabbit anti-aPKC (C-20 Santa Cruz 1:1000).

In vitro kinase assay
GST-Baz fragments GST-Baz N1 (aa 1-280), GST-Baz N2 (aa 281-736), GST-Baz N3 (aa 737-1124), GST-Baz N4 (aa 1125-1464), GST-Myosin Light Chain (MLC) WT (*Gallus gallus* Regulatory Myosin Light Chain 9), and GST-$MLC^{T19A,S20A}$ were expressed and purified from *E.coli.* 30 pmol of purified proteins were incubated with 5 pmol of recombinant human GST-ROCK2 CA (Cell Signaling) in kinase buffer containing 50 mM Tris-HCl at pH 7.5, 5 mM MgCl2, 1 mM EDTA, 1 mM EGTA, 1 mM DTT, 0.1 mM γ-[^{32}P]-ATP (20 GBq/mmol). After 1 h incubation at 30ºC, the reaction was terminated by boiling 5 min in SDS sample buffer and equivalent portions of each sample were subjected to SDS-PAGE.

Lipid-binding assay
In vitro kinase assays were performed as described above, using GST or GST-Baz N4 as substrates and cold ATP. Y-27632 was added at 1 mM, where indicated. The reactions were terminated by addition of blocking solution (PBS + 1% nonfat milk) to a final concentration of 0.25 μg/ml for each substrate and incubated with Lipid strips containing spots of different phosphoinositide membrane lipid composition (Echelon Biosc., Inc.). The Lipid strips were then washed and probed with antibodies against GST (Sigma) using standard western blot procedures.

SUPPLEMENTAL REFERENCES

Chou, T. B. and Perrimon, N. (1996). The autosomal FLP-DFS technique for generating germline mosaics in *Drosophila melanogaster*. Genetics *144*, 1673-1679.

Fanto, M., Weber, U., Strutt, D. I. and Mlodzik, M. (2000). Nuclear signaling by Rac and Rho GTPases is required in the establishment of epithelial planar polarity in the *Drosophila* eye. Curr Biol *10*, 979-988.

Krahn, M. P., Klopfenstein, D. R., Fischer, N. and Wodarz, A. (2010). Membrane targeting of Bazooka/PAR-3 is mediated by direct binding to phosphoinositide lipids. Curr Biol *20*, 1-7.

Wang, Y. and Riechmann, V. (2007). The role of the actomyosin cytoskeleton in coordination of tissue growth during *Drosophila* oogenesis. Curr Biol *17*, 1349- 1355.